Cosmic Masers: Proper Motion toward the Next-Generation Large Projects
Proceedings IAU Symposium No. 380, 2024
T. Hirota, H. Imai, K. Menten, & Y. Pihlström, eds.
doi:10.1017/S1743921323003551

Maser polarization simulation in an evolving star: effect of magnetic field on SiO maser in the circumstellar envelope

M. Phetra[1,2], M. D. Gray[2], K. Asanok[2], B. H. Kramer[2,3], K. Sugiyama[2], S. Etoka[4] and W. Nuntiyakul[5]

[1]Graduate School, Chiang Mai University, Chiang Mai 50200. email: montree_ph@cmu.ac.th

[2]National Astronomical Research Institute of Thailand, Chiang Mai 50180, Thailand

[3]Max Planck Institute for Radio Astronomy, Auf dem Hügel 69, Bonn 53121, Germany

[4]Jodrell Bank Centre for Astrophysics, School of Physics and Astronomy, University of Manchester, M13 9PL, UK

[5]Department of Physics and Materials Science, Faculty of Science, Chiang Mai University, Chiang Mai 50200, Thailand

Abstract. Maser polarization changes during a pulsation in the CSE of an AGB star are related in a complicated way to the magnetic field structure. 43 GHz SiO maser transitions are useful for polarization study because of their relatively simple Zeeman splitting structure and their location. This work uses 3D maser simulation to investigate the effect of the magnetic field on maser polarization with different directions. The results show that linear polarization depends on the magnetic direction while circular polarization is less significant. The EVPA changes through $\pi/2$ at an angle of around 50 degrees, approximately the Van Vleck angle. The EVPA rotation result from 3D maser simulation is consistent with results from 1D simulations, and may explain the 90 degree change of the EVPA within a single cloud in the observational cases of TX Cam and R Cas.

Keywords. AGB star, maser polarization, maser simulation

1. Introduction and Method

The pulsation of CSE in an AGB star is a puzzling process, with its properties varying periodically. VLBI observations show that maser intensity and polarization in this region significantly change during pulsation. A model of the pumping process is required to help us understand the physical mechanisms behind the phenomenon of maser variability. Goldreich *et al.* (1973) showed that the magnetic field may be one of the physical conditions controlling polarization because of the Zeeman splitting effect, especially in a molecule with weak Landé splitting factors in its quantum states. The SiO molecule is a good maser polarization candidate because it is located closest to the AGB star with a strong magnetic field present (Vlemmings 2019). Observations of SiO masers at transition mode v=1, J=1-0 (43 GHz) may show a nonuniform polarization and 90-degree flip (Assaf *et al.* 2013; Tobin *et al.* 2019). Here, we consider the effect of magnetic field on maser clouds by using 3D maser polarization simulation which is modified from Gray *et al.* (2018).

The maser simulation starts with a density matrix (DM) as a function of time, position, and Doppler velocity. The DM is used to determine the population of energy levels

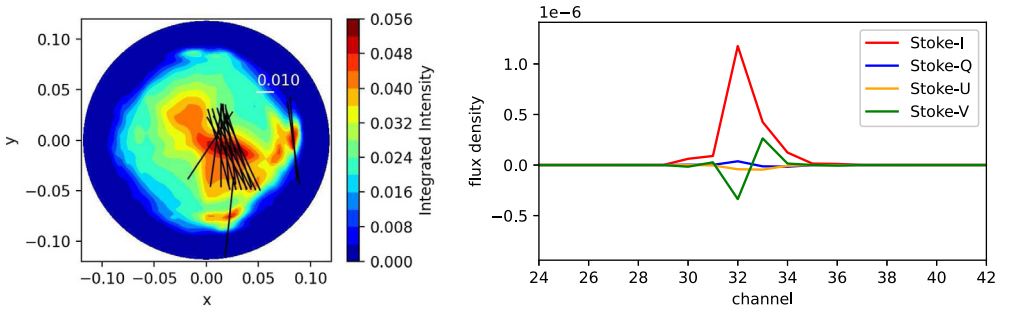

Figure 1. Stokes-I map with EVPA and Spectra of the depth multiplier = 300 for parallel MFD.

which are controlled by a Hamiltonian operator containing a magnetic perturbation, an interaction with the electric field, and an additional decay rate. Then, we use a spherical distribution of background rays, each with 2 electric field components to evolve the DM into an increasingly saturated state by using the radiative transfer equation. Finally, we amplify rays from a plane background that pass through the known DM in the observer's direction for the formal solution as image intensities and spectra.

In this work, we set the domain as a multi-node spread in one cloud with a cylindrical shape to calculate the DM. The magnetic field is applied to the domain in different directions from parallel to perpendicular with the z-axis in steps of 5 degrees. Then we have 19 solutions with different magnetic field directions (MFDs). Then, the depth multiplier is used to optically thicken the model (Phetra *et al.* 2023) until the inversions are close to 0. Finally, formal solutions from the plane background are converted to observer's Stokes parameters.

2. Results

The important simulation parameters are set by the Zeeman splitting as $g\Omega = 0.7405\,\mathrm{s}^{-1}\,(\mathrm{mG})^{-1}$, decay rate as $\Gamma = 5\,\mathrm{s}^{-1}$, the ratio of the background intensity to the saturation intensity as 10^{-6} (Western & Watson 1984), and the magnetic field strength $B = 10^4$ mG (Herpin *et al.* 2006; Diamond *et al.* 1997) (the splitting width become $7405\,\mathrm{s}^{-1}$ and use this value for a channel width). We solve for the DM in a range of depth from 3 to 300 (in steps of 3) using the spherical radiation background with a radius of 5 domain units. For formal solutions, the plane radiation background is behind the domain by 5 units, and radiates towards the distant observer who is 1000 units in front of the domain. The example result for the observer which comes from the tube domain with parallel field is shown in Figure 1 as Stokes-I map with their EVPA and spectra.

In the Stokes-I map, color contours refer to the integrated intensity (saturation units) from all frequency channels, and the EVPA (EVPA $= 0.5\arctan(U/Q)$) of each ray is shown in a black solid line with the length represented by Stokes-I shown at the upper-right of the image, the highest integrated intensity is about 0.056. For spectra, we plot all Stokes parameters at different colors shown in the upper-right of the image. The spectra of Stokes-Q and U look small while Stokes-V clearly shows the s-shape.

The rays from the spherical background in the 3D simulation each have an electric field with a uniformly distributed random phase and a normally distributed random amplitude. This means that random features can propagate through a series of solutions at increasing values of the depth multiplier. Therefore, we make an exponential fit to the integrated flux as a function of the depth multiplier to match the general trend. The fitting parameters are used to calculate the polarization properties consisting of fractional linear polarization ($m_l = \sqrt{Q^2+U^2}/I$), fractional circular polarization ($m_c =$

https://doi.org/10.1017/S1743921323003551 Published online by Cambridge University Press

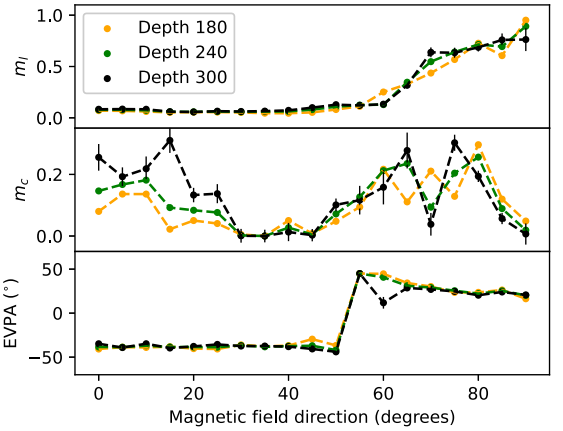

Figure 2. m_l, m_c, and EVPA with their residual values as a function of MFD for a depth multiplier 180, 240, and 300.

$|V|/I$), and EVPA. Polarization properties of each domain, at a set of depths, are plotted as a function of the MFD in Figure 2. The black vertical line at each simulation MFD represents the standard error of the computed value with respect to the fitted exponential. Uncertainty on m_l, m_c, and EVPA were obtained by standard error propagation.

The value of m_l increases rapidly from 0.13 to 0.64 over the MFD range of 60 to 70 degrees while m_c fluctuates in the range of 0.00 to 0.30. We found that the EVPA is suddenly changed at the MFD of 50 to 55 degrees from -44° to 45°.

3. Discussion and Conclusions

We use the 3D maser polarization simulation to explain the effect of MFD in CSE. The preliminary results show that the polarization properties depend on the direction of the magnetic field, as expected from 1D models. When the magnetic field is parallel with z-axis, Stokes-V shows a negative value at the low frequency, and a positive value at high frequency (Nedoluha & Watson 1994). This result agrees with 1D results in Tobin *et al.* (2023).

For the comparison of polarization properties with MFD, we found that m_l is low at low angles and then increases after a MFD of about 60 degrees while the 1D model in Tobin *et al.* (2023) shows that m_l is larger at low angles. We found a nonzero in circular polarization which the fractional is about 0.3, similar to the 1D model with a magnetic field strength of 10 G. However, Watson & Wyld (2001) and Tobin *et al.* (2023) show the dependence of unitless of circular polarization on MFD, θ, as $v/(pB\partial i/\partial v) = \cos\theta$, we need to check this relation base on our 3D simulation results. We found that the fractional polarization results look similar to the observations such as Assaf *et al.* (2012) and Kemball & Diamond (1997). Moreover, we found that the flip of EVPA is dominated by a Stokes-Q flip at the MFD of 50 to 55 degrees which is similar to the result of Goldreich *et al.* (1973) in case 2a.

We made a new domain with 2 different MFDs internally to test whether the EVPA flip in one cloud that has been detected in observations can also be generated by our simulation. The MFDs are set as 15 degrees for the lower part and 75 degrees for upper part of the domain. We compare the result with the EVPA flip observed from TX Cam (Tobin *et al.* 2019) and shown in Figure 3.

We found that the EVPA from the lower part is close to 0° while in the upper part, the direction is about -23°. So, the field variation in this new domain leads to results that are consistent with the observed EVPA change. Georgiev *et al.* (2023) monitors R

https://doi.org/10.1017/S1743921323003551 Published online by Cambridge University Press

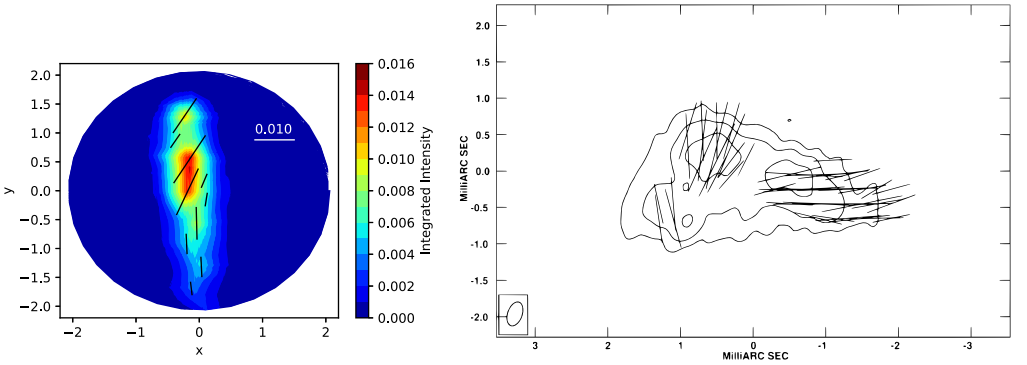

Figure 3. A new domain with different directions of a magnetic field in a single cloud compare with EVPA change in TX Cam (Tobin *et al.* 2019).

Sct in the wavelengths between 375 to 1050 nm and found that the surface magnetic field in the CSE was detected at different phases of pulsation and suggests that this may be caused by the pulsation shock wave. However, the goal of this project is to attempt to model the global magnetic field during a pulsation, so, we need to test more complicated cases, such as multi-clouds, anisotropic pumping, and the motion cloud.

References

Assaf, K. A., Diamond, P. J., Richards, A. M. S., & Gray, M. D. 2012, *IAU Symposium*, 287, 235

Assaf, K. A., Diamond, P. J., Richards, A. M. S., & Gray, M. D. 2013, *MNRAS*, 431, 1077

Diamond, P. J., Kemball, A. J. & Boboltz, D. A., 1997, *Vistas in Astron.*, 41, 175

Georgiev, S., Lèbre, A., Josselin, E., Mathias, P., Konstantinova-Antova, R., & Sabin, L. 2023, *MNRAS*, 522, 3861

Goldreich, P., Keeley, D. A., & Kwan, J. Y. 1973, *ApJ*, 179, 111

Gray, M. D., Mason, L., & Etoka, S. 2018, *MNRAS*, 477, 2628

Herpin, F., Baudry, A., Thum, C., Morris, D., & Wiesemeyer, H. 2006, *A&A*, 450, 667

Kemball, A. J., & Diamond, P. J. 1997, *ApJ*, 481, L111

Nedoluha, G. E., & Watson, W. D. 1994, *ApJ*, 423, 394

Phetra, M., Gray, M. D., Asanok, K., Kramer, B. H., Sugiyama, K., Chanapote, T., & Nuntiyakul W. 2023, *J Phys Conf Ser*, 2431, 012088

Tobin, T. L., Kemball, A. J. & Gray, M. D. 2019, *ApJ*, 871, 189

Tobin, T. L., Gray, M. D. & Kemball, A. J. 2023, *ApJ*, 943, 123

Vlemming, W. 2019, *IAU Symposium*, 343, 19

Watson, W. D. & Wyld, H. W. 2001, *ApJ*, 558, L55

Western, L. R., & Watson, W. D. 1984, *ApJ*, 285, 158

https://doi.org/10.1017/S1743921323003551 Published online by Cambridge University Press

Review talk in the session Theory of Masers and Maser Sources by Martin Houde. Taken by Tomoya Hirota.

https://doi.org/10.1017/S1743921323003551 Published online by Cambridge University Press